The Monterey Area Ship Track Experiment

PHILIP A. DURKEE

Department of Meteorology, Naval Postgraduate School, Monterey, California

KEVIN J. NOONE

Stockholm University, Stockholm, Sweden

ROBERT T. BLUTH

Office of Naval Research, Arlington, Virginia

(Manuscript received 14 November 1996, in final form 23 February 1999)

ABSTRACT

In June 1994 the Monterey Area Ship Track (MAST) experiment was conducted off the coast of California to investigate the processes behind anthropogenic modification of cloud albedo. The motivation for the MAST experiment is described here, as well as details of the experimental design. Measurement platforms and strategies are explained, and a summary of experiment operations is presented. The experiment produced the largest dataset to date of direct measurements of the effects of ships on the microphysics and radiative properties of marine stratocumulus clouds as an analog for the indirect effects of anthropogenic pollution on cloud albedo.

1. Introduction

Determining the effects of atmospheric aerosol particles on the radiative balance of the earth has been a major focus of recent climate research. Aerosols can influence the earth's heat balance directly by reflecting some of the incoming solar radiation back to space, reducing the amount of energy reaching the earth's surface. Aerosols can also indirectly influence the radiation budget by inducing changes in the radiative properties of the clouds that form on them. Currently, the magnitude of this indirect radiative effect of aerosols is regarded as one of the greatest uncertainties in climate forcing (Charlson et al. 1992; Hansen et al. 1995). A recent report from the Intergovernmental Panel on Climate Change lists estimates of the globally and annually averaged anthropogenic radiative forcing of greenhouse gases and aerosols (Houghton et al. 1996). The global mean anthropogenic radiative forcing due to greenhouse gases was estimated at a high confidence level to be $+2.5$ W m^{-2}. Estimates of the magnitude of the indirect radiative effect of tropospheric aerosols were so uncertain that no central value was given in the report; however, the upper limit of the indirect aerosol forcing estimate was -1.5 W m^{-2}. Clearly, reducing the uncertainty in, or even arriving at, a central value for the estimates of the indirect radiative effect of aerosols is a prerequisite for making progress on understanding human influences on climate.

Thirty years ago, curvilinear cloud structures were observed in visible-wavelength satellite images from the early Television Infrared Observational Satellites (TIROSs) (Conover 1966). In these earliest images, the ''anomalous cloud lines'' were suspected to have been caused by aerosol particles produced by ships (Conover 1966; Twomey et al. 1968) and have subsequently been called ship tracks. More recent observations have strengthened the link between ships and ship tracks (Radke et al. 1989; Ferek et al. 1998). While the early observations in the TIROS images were limited to the visible region of the spectrum, recent measurements at near-IR wavelengths reveal more extensive signatures of ship effects on clouds (Coakley et al. 1987). These new observations of ship tracks from space have prompted interest in the processes that form ship tracks. The fundamental motivation for investigating the ship track phenomenon is to understand the basic atmospheric problem of how anthropogenic aerosols modify the reflectivity of clouds and potentially the earth's radiation balance.

Ship tracks provide us with a unique opportunity to investigate the processes behind the indirect radiative

Corresponding author address: Prof. Philip A. Durkee, Department of Meteorology, Naval Postgraduate School, 589 Dyer Road, Monterey, CA 93943-5113.
E-mail: durkee@nps.navy.mil

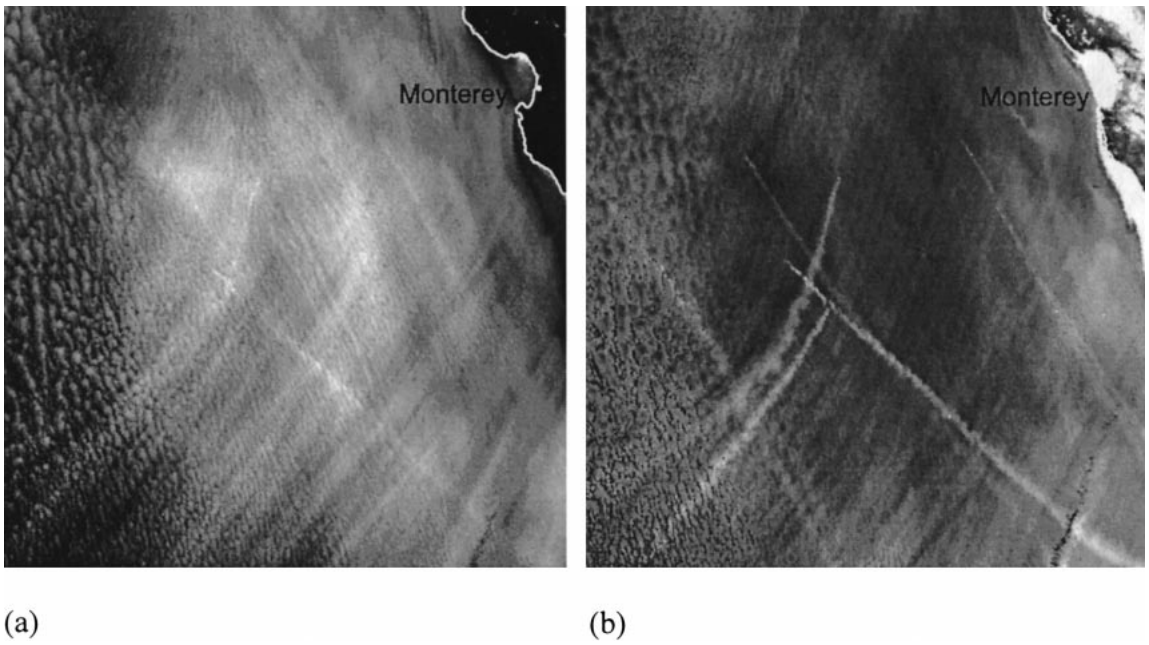

FIG. 1. *NOAA-9* AVHRR satellite images. (a) Channel-1 (0.63-μm wavelength) and (b) channel-3 (3.7-μm wavelength) images of the MAST operating area on 27 Jun 1987 at 1753 UTC.

effect of aerosols since they are a particular manifestation of the more general problem of the influence of anthropogenic pollution on cloud albedo. The fact that anthropogenic pollution could influence the reflectivity of clouds has been recognized for some time (Twomey 1974; Charlson et al. 1987; Albrecht 1989). It has proven to be extremely difficult to directly assess the radiative impact of aerosols on clouds (and the climatic consequences of the effect) from remote sensing measurements alone (e.g., Schwartz 1988; Falkowski et al. 1992; Kim and Cess 1993; Han et al. 1994). One of the principal difficulties in these previous studies has been to extract a signal in changes in cloud albedo or effective radius due to anthropogenic pollution from a multitude of sources on continental, or even hemispheric, scales. Due to the large spatial and temporal scales involved in these previous studies, they have been confronted with the difficulty of having different background conditions and dynamic driving forces for the clouds in the areas that were observed. In addition, the clouds in which this indirect radiative effect would manifest itself generally exhibit a high degree of natural variability, which will mask the aerosol influence.

The advantage of investigating ship tracks as an analog to anthropogenic pollution in general is that one has an isolated, individual source (a ship) in a relatively simple environment (the stratocumulus-topped marine boundary layer). We have the possibility of characterizing both the source and the background in a comprehensive manner with both in situ and remote sensing measurements. We can investigate cases where we have a specific source in the marine boundary layer causing a specific, observed change in cloud albedo—an easily identified localized perturbation of an extensive cloud system. Ship tracks provide us with an opportunity to design as controlled an experiment as we are likely to achieve in the real atmosphere to investigate the processes underlying the indirect radiative effect of aerosols on clouds.

As an example of ship tracks, Fig. 1 shows images of clouds off the coast of central California taken from the *NOAA-9* satellite. Figure 1a is a visible wavelength (0.63 μm) advanced very high resolution radiometer (AVHRR) channel-1 image, and Fig. 1b is the coincident near-infrared wavelength (3.7 μm) AVHRR channel-3 image collected on 27 June 1994. Both images show extensive stratocumulus cloud layers. A number of ship tracks are apparent in the image, many of which extend for hundreds of kilometers. The tracks persist for timescales of up to a day, perhaps even somewhat longer. Note that the ship track signatures are much more apparent in the near-infrared wavelengths.

The difference between the two wavelengths is primarily due to moderate absorption of near-infrared radiation by cloud droplets, while clouds only weakly absorb visible radiation. The reflectance of clouds at visible wavelengths is determined by cloud thickness, liquid water content, and cloud droplet size distribution. The absorption at near-infrared wavelengths is strong enough to limit the penetration of incoming solar photons to less than about 100 m. As a result, for typical cases of marine stratiform clouds greater than about 100 m thick, the reflectance at 3.7 μm is determined almost exclusively by the cloud droplet size distribution. There-

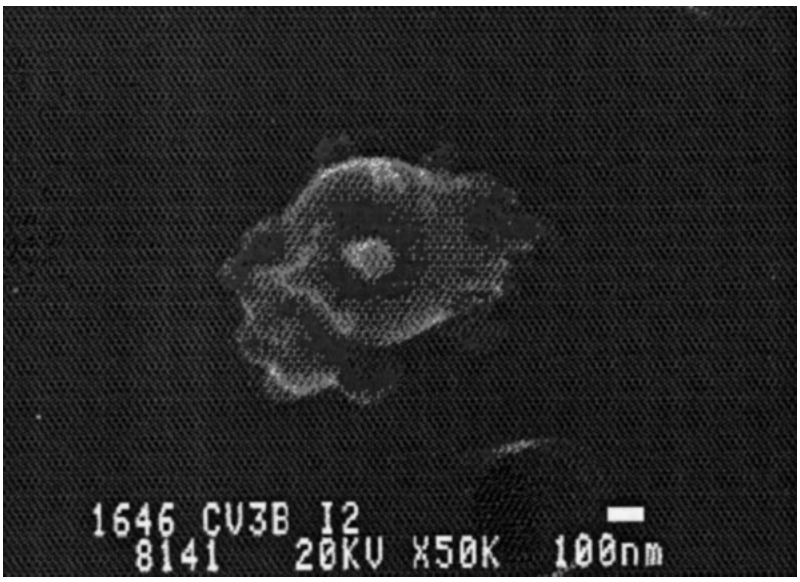

FIG. 2. Scanning electron microscope image of a combustion-derived particle collected in the USS *Mount Vernon* plume on 27 Jun.

fore, the reflectance pattern of the clouds in Fig. 1a at a visible wavelength is highly variable because of changes in cloud thickness, liquid water content, and droplet size changes due to various dynamical and microphysical effects in cloud formation. For some ships, the perturbation to the cloud is sufficient to be detectable at visible wavelengths. For many more ships, since the aerosol effluent primarily affects the droplet size distribution, the perturbation of the cloud is only apparent at the 3.7-μm wavelength.

The working definition of a ship track for the Monterey Area Ship Track (MAST) science team is based on appearance in satellite imagery. Although ship tracks are observed in both visible and near-infrared imagery, many more ship tracks appear in the near-infrared, and it is rare that a ship track feature is apparent in visible imagery alone. The definition of a ship track is therefore taken from its near-infrared signature. A ship track is a curvilinear, bright feature in mid-IR imagery that is spatially coincident with the effluent plume of a ship. Due to turbulent diffusion, a ship track typically broadens from 1 to 2 km at the so-called head to widths of tens of kilometers down track. Ship tracks have been observed to be up to several hundred kilometers long. A complete description of ship track characteristics is given in Durkee et al. (2000b).

It can be seen from the satellite images that the ship track effect manifests itself on very large spatial scales and for long periods of time. The underlying processes causing the effect, however, have different spatial and temporal scales. Figure 2 is a scanning electron microscope image of a combustion-derived particle that was found in the plume of the USS *Mount Vernon,* one of the ships investigated on 27 June. The particle is below 0.5 μm in radius. The cloud droplets in the ship tracks themselves on this day were typically 6–7 μm in radius. Aerosol particles activate and grow to cloud droplet size on timescales of seconds or less. The differences in temporal and spatial scales of the effects of aerosols on cloud albedo and the processes causing the effects present a real challenge in terms of both measuring and modeling the system in question.

The importance of the issue of cloud albedo modification due to anthropogenic pollution, as well as the sparseness of measurements in ship tracks and the lack of knowledge about the processes generating them, were major driving forces behind the MAST program.

This paper serves as an overview of the objectives, experimental design, and execution of MAST. A discussion of previous ship track studies is followed by the experimental design. The platforms and measurement capabilities are described, and a summary of MAST operations completes the body of the paper. The papers that follow in this special issue will therefore not repeat the detailed information presented here.

2. Previous track studies: What was known prior to MAST

Prior to MAST, perhaps the least understood aspect of ship tracks was exactly which combination of effluents generated by the ship contribute to ship track formation. We use the term effluent in this context to include the entire range of perturbations induced by the ship: particulate and gaseous emissions, heat, and mechanical turbulence generated by the ship. There are at least three likely sources of particulate effluents. One source could be particles emitted directly from the ship's stack. Another possibility is sea-salt particles generated in the ship's wake. Yet a third possibility is particles

produced after the oxidation of sulfur dioxide or another of the gases emitted by the ship. Determining the source of the ship-generated aerosol particles causing nucleation of droplets in ship tracks was the major theme of the MAST experimental design.

Not every ship causes a ship track. Ship tracks are seldom (if ever) observed in some geographical locations, while they are prevalent in others. Clearly, there must be a combination of ambient conditions necessary in the marine atmosphere before ship tracks will form. Conover (1966) and Bowley (1967) suggested several conditions from early observations from TIROS satellites. The conditions suggested were 1) a shallow, cloud-topped, well-mixed boundary layer; 2) a low number of background cloud condensation nuclei (CCN); and 3) a relatively narrow range of temperature and relative humidity values at the surface. This list may not be exhaustive. There may well be other important conditions necessary for ship track formation. Observing these conditions was another focus of MAST. Determining the set of conditions necessary for ship tracks to form will hopefully give us clues as to where, when, and to what extent we may be able to observe the radiative influence of atmospheric aerosols on cloud albedo.

a. Image analysis

Satellite observations have strengthened the ship effluent and cloud albedo relationship. Conover (1966) described anomalous ''cloud lines'' as clouds generated by ship passage. These features are observable in visible-wavelength satellite images as long, narrow, linear clouds. However, ship effects are more frequently observed at near-infrared wavelengths as modifications to preexisting stratiform clouds.

Coakley et al. (1987) first described this infrared ''ship track'' signature through satellite observations made with National Oceanic and Atmospheric Administration (NOAA) AVHRR. At the 3.7-μm wavelength (channel 3) ship tracks are characterized as long, narrow, curvilinear features that have a greater albedo than the surrounding cloud cover. Following this paper, Radke et al. (1989) and King et al. (1993) presented measurements from aircraft in a ship-influenced cloud. These observations showed that cloud microphysical effects were important for the formation of tracks observed at 3.7-μm wavelength. In their aircraft measurements, they found an increase in cloud droplet number and a decrease in cloud droplet size. It was the decrease in droplet size that produced the increase in cloud albedo that is observed at 3.7-μm wavelength as a ship track.

The 27 June images depicted in Fig. 1 show a large areal cloud cover. Examination of many other images indicates the amount of susceptible cloud cover is the primary reason for the large number of ship tracks evident on the 27 June image.

Table 1 summarizes qualitative results of satellite observations of ship tracks worldwide. Ship tracks have been observed in all the regions listed in the table. Not all regions have been inspected equally, but it is apparent that ship tracks are observed in many oceanic areas. Most stratus regions over eastern oceans exhibit tracks, and ship track occurrence increases generally with increasing latitude coincident with increased stratus cloud cover.

TABLE 1. Oceanic regions where ship tracks have been observed in AVHRR imagery.

Oceanic region	X > 20 observed	Comments
Barents Sea		Mid–warm season; high sun; lower winds
Bering Sea	X	Same with stronger sun angle dependence
Davis Strait	X	Limited observation; mid–warm season; high sun
Denmark Strait	X	Limited observation; mid–warm season; high sun
East North Atlantic Ocean	X	Tracks all seasons; warm-season dominant
East North Pacific Ocean	X	Tracks all seasons, but bias to warm season
East South Pacific Ocean	X	Limited observation; warm-season peak occurrence
East China Sea		Very rare, cool-season phenomenon
Greenland Sea	X	Primarily warm-season, high-sun phenomenon
Gulf of Alaska	X	Tracks primarily warm-season feature and high-sun elevation; winter also
Gulf of California		Stratus very rare; few tracks observed only once; cool season
Kara Sea		Mid–warm season; high sun; lower winds
North Sea	X	Primarily warm season; clean air masses
Norweigian Sea	X	Primarily warm-season, high-sun phenomenon
Sea of Japan	X	Early warm-season peak with clear air masses
Sea of Okhotsk	X	Tracks primarily warm-season feature with peak early summer; cool SST; low wind
South Atlantic Ocean	X	Tracks all season; warm-season dominant
Tasman Sea		Limited observation
Yellow Sea		Very rare, cool-season phenomenon

Ship tracks have been found to form in very diverse stratiform cloud types and marine atmospheric boundary layer (MABL) conditions (Evans 1992; Millman 1992). MABL conditions that have been observed to be susceptible to ship track formation are fog, stratus, and stratocumulus with layer depths ranging from very shallow up to 1400 m. Ship tracks have also been observed in coupled and decoupled boundary layers (boundary layers where the overlying stratocumulus cloud deck is either entirely decoupled from surface fluxes or partially coupled to the surface layer through cumulus clouds). This is surprising since in a decoupled boundary layer the internal stable layer should inhibit the transport of

ship effluent from the surface to the cloud, or at least cause the transport rate to be slower and more inhomogeneous.

The dominant areas of stratiform clouds are the eastern ocean basins between 20° and 50° latitude (off the west coasts of continents), and at high latitudes above about 60°N and S. Overall, stratiform clouds cover 25%–30% of the world's oceans. It is important to note that stratus clouds also form outside these favored regions. The hypothesized formation processes are not expected to limit formation to specific regions, beyond the need for cloud systems ''connected'' to the surface by a transport mechanism. Therefore, it is expected the ships can perturb stratiform clouds in all regions of the world when the conditions exist for low-lying clouds.

The formation characteristics of stratiform clouds show significant seasonal variation. For the eastern-ocean, subtropical stratus systems, the months of May–September represent the maximum period of stratus formation. However, stratus and ship tracks form in all months of the year.

Ship tracks are also observed at night (Kuciauskas et al. 1993). Ship tracks are apparent in 3.7-μm wavelength images at night because of reduced emittance from the smaller droplet distribution in the track relative to the ambient cloud. At longer wavelengths clouds become blackbodies for all droplet sizes, and the tracks do not emit differently than the ambient clouds.

The persistence of the stratiform clouds may also play a role in the number of tracks detected for a given location and area of cloud. However, ship tracks disappear as the cloud droplet size in the tracks grows to match the average drop size in the unperturbed clouds, which eventually causes the albedo of the ship track to reach equilibrium with the surrounding cloud. The time frame for this process is partially addressed in MAST results, and may be dependent on ship-generated aerosols, relative wind to the ship, and precipitation state of the cloud. However, ship tracks have been known to persist for up to two days.

b. In situ measurements

Radke et al. (1989) and King et al. (1993) describe the first in situ measurements of ship tracks. The tracks were encountered off the southern California coast in 1987. The University of Washington (UW) C-131A aircraft flew through the tracks unintentionally so only one pass of data is available. The measurements show increases in droplet numbers and decreases in droplet sizes. The observations also showed that, at least in this case, liquid water content of the cloud increased (2–3 times in this case).

Hindman and Bodowski (1994) reported a well-defined cloud line produced by an unidentified steaming ship detected in satellite imagery and simultaneously photographed from the R/V *Egabrag III*. The *Egabrag* itself produced a much less well-defined cloud line. Measurements made from the *Egabrag* revealed that the cloud lines formed in a shallow boundary layer that was nearly saturated, unstable, drizzling, and nearly free of CCN. The *Egabrag* passed through the plume of the ship as indicated by elevated CCN concentrations coincident with the cloud line. Thereafter, both ships passed under a shallow stratus layer where background CCN concentrations increased significantly. The cloud line produced by the passing ship extended into the stratus layer, but the *Egabrag* did not affect the stratus layer. Production of the cloud lines appeared dependent on a combination of environmental conditions and ship effluent.

Ferek et al. (1998) obtained in situ measurements in two ship tracks observed in satellite imagery off the coast of Washington State. They concluded that the CCN emitted from the ships was responsible for the decrease in the observed cloud drop size in the tracks.

c. Summary of previous studies

The broad conceptual links between anthropogenic pollution, cloud microphysics, and cloud albedo first advanced by Twomey et al. (1968) were largely confirmed by the few coupled in situ and remote sensing studies carried out prior to MAST. The fact that the albedo changes in the few available observations were caused by an increase in droplet number concentration and a decrease in droplet size agreed qualitatively with theoretical expectations. The concurrent increase in aerosol and CCN concentrations in the few observed ship tracks were an indication that aerosols were at least part of the cause of the microphysical perturbations, but other effects (e.g., turbulence, heat, and moisture injection) could not be eliminated. Due to the scarcity of observations, it was impossible to assess what background boundary layer conditions were necessary for ship track formation.

What was perhaps most lacking prior to the MAST experiment was a complete set of data that would allow us to elucidate the mechanisms and processes behind ship track formation. There was also very little information available with which to quantify the relationship between the strength of the perturbation due to a ship, the magnitude of the microphysical changes induced in the perturbed areas of clouds, and the resultant values of changes in cloud albedo. MAST was aimed at obtaining information with which we could begin to remedy these deficiencies.

3. Scientific plan

Before presenting the specific hypotheses we wished to test with the MAST experiment, we will illustrate some of the problems associated with an experimental investigation of the indirect radiative effect of aerosols with a hypothetical case of cloud formation in the marine boundary layer.

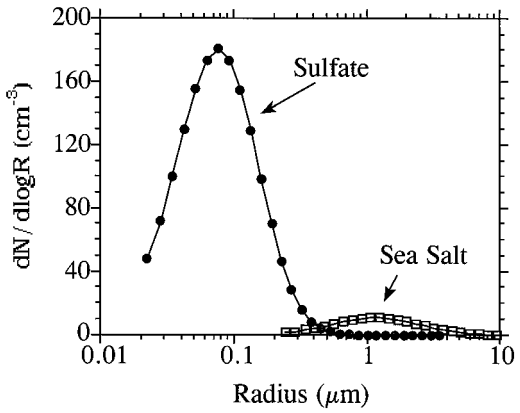

FIG. 3. Model input aerosol number size distributions with particles from two sources; sulfate and sea salt. Particle concentrations are 133 cm^{-3} for sulfate and 9 cm^{-3} for salt.

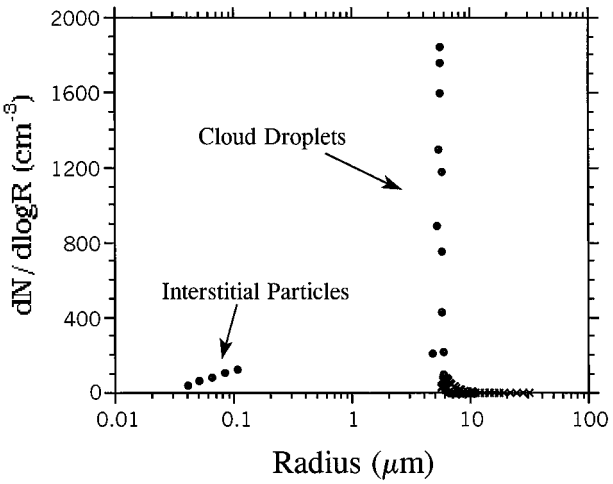

FIG. 4. Size distributions after cloud formation. Size distributions of interstitial aerosol particles and cloud droplets 28 m above cloud base. The updraft velocity was fixed at 40 cm s^{-1}. The number of activated cloud droplets was 92 cm^{-3} and the liquid water content was 69 mg m^{-3}.

a. An example of aerosol–cloud interactions and cloud microphysics

Figure 3 is a conceptual diagram of how different chemical species may be distributed across the ambient aerosol size spectrum in the boundary layer, and how the distribution is related to particle sources. Number size distributions of particles from two sources (sulfate and sea salt) are shown. The curves were generated using a kinematic, Lagrangian parcel model that has explicit cloud microphysics and size-resolved aerosol and droplet chemistry (Ayers and Larson 1990). They represent typical marine aerosol size distributions in the remote boundary layer below cloud. Sulfate particles in the marine atmosphere tend to be found primarily in the submicrometer part of the aerosol size spectrum, while a large fraction of the sea-salt particle mass is found in the supermicrometer fraction. When particles from two such sources are combined, there is a size range of the new mixed aerosol that contains both sulfate and sea-salt particles.

In the marine environment, supersaturation values may be such that most, but not all, of the aerosol particles will nucleate cloud droplets. In this case, the smallest fraction of the aerosol (and perhaps some larger hydrophobic particles as well) will be left in the interstitial aerosol. The process of nucleation scavenging (cloud formation) is illustrated in Fig. 4. In this model run using an updraft velocity of 40 cm s^{-1}, particles larger than 0.104 μm grew to form cloud droplets, while particles smaller than this size remained in the interstitial air. At 1038 m (28 m above cloud base), the cloud droplet number concentration was 91 cm^{-3}. In this case, 64% of the total number of aerosol particles were activated into cloud droplets. All of the salt particles grew into droplets, as did 68% of the sulfate particles. The sulfate particles smaller than a 0.104-μm radius remained in the interstitial reservoir.

Entrainment and other effects may tend to smear out the sharp cut caused by nucleation scavenging. A higher updraft velocity would generate higher peak supersaturation values, nucleating more of the smaller particles. Additionally, the chemical composition of the particles can influence their droplet nucleating ability. The purpose of the model run presented here was not to simulate any particular cloud or cloud type, but rather to illustrate the nucleation process. An important aspect of the model results is that the residual (scavenged) aerosol may consist of particles from different sources, the proportions of which will depend upon source strength and scavenging processes. Determining the aerosol particles that cause ship tracks will depend in part on being able to identify the droplet residual particle composition.

Particles emitted by a ship may directly influence the CCN population in the marine atmosphere. Whether the CCN cause a perturbation in the spectral reflectance of the cloud will depend upon a number of factors. If the particles are very small, the supersaturation required for them to become activated and grow may not be attainable in marine clouds. They would then remain as interstitial particles in the cloud. If the particles were sufficiently large, they could be large enough to nucleate cloud droplets and modify cloud albedo. There are, however, conditions under which even relatively large particles may not nucleate cloud droplets. Hydrophobic or insoluble particles of a given size are less likely to nucleate droplets than their soluble counterparts, which introduces a chemical influence on droplet nucleation. If there were a large number of particles present in the interstitial reservoir in the cloud, then adding more from the ship may not have any influence on droplet number in the cloud since there would already have been an overabundance of particles upon which droplets could nucleate (Leaitch et al. 1992; Noone et al. 1992). Quantifying, understanding, and modeling the effects of di-

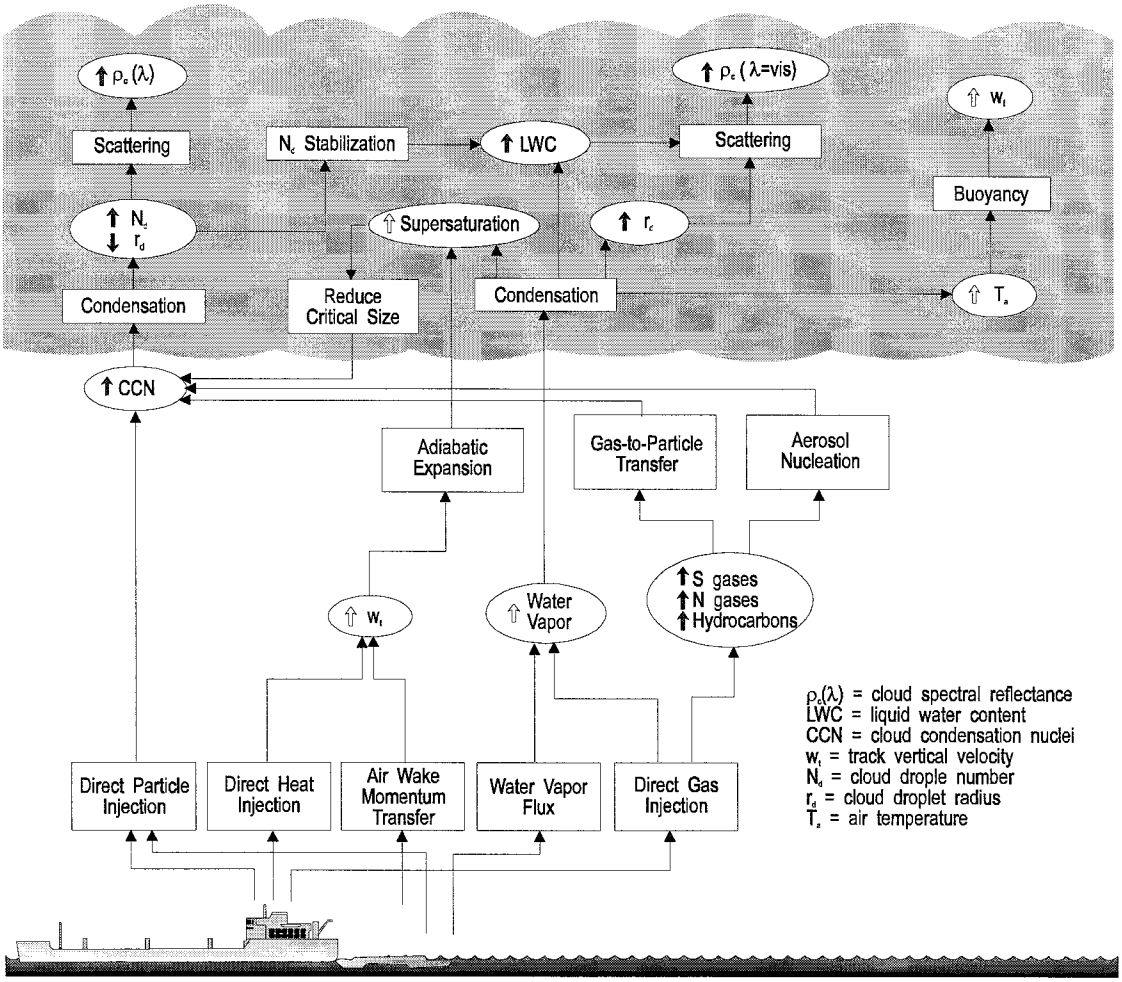

FIG. 5. Schematic representation of the hypotheses of ship track formation in the near-ship environment. Rectangles represent processes and ovals indicate the effect (up arrows for an increasing and down arrows for a decreasing effect) of the process on a specific constituent. The solid arrows indicate the constituent change has been observed in aircraft, ship, or satellite measurements.

rect particle injection on cloud spectral reflectance require investigating all of the above processes.

Gases such as NO and SO_2 are also emitted by ships. If there is sufficient oxidant present in the atmosphere, these gases can be converted to HNO_3 (nitric acid) and H_2SO_4 (sulfuric acid). If sulfuric acid is produced from the ship's effluent, it can subsequently either form new aerosol particles, or condense on particles or droplets already present.

It is generally thought that new particle production (gas-to-particle conversion) would not occur in clouds due to the large droplet surface area available upon which the H_2SO_4 vapor could condense. Recent model calculations, however, have indicated that new particle production in cloud may happen under some conditions (Hegg 1991). Even if new particles were produced, they would initially be too small to influence the CCN population in the immediate vicinity of the ship. They would have to grow or coagulate to larger sizes before they could themselves nucleate new cloud drops. Any influence of freshly produced particles on cloud albedo would have to occur down track after sufficient time had elapsed for particle generation processes to occur.

Another possible sink for sulfuric acid vapor is for it to condense onto particles already present in the atmosphere, particularly below cloud. This process could modify the CCN population by causing already-existing particles (which were either too small or which had the wrong chemistry to be CCN) to become able to nucleate cloud droplets. The occurrence of this process, and whether it happens near or away from the ship, will depend upon airborne oxidant concentrations, SO_2 emissions, and particle concentrations. If the process were active, it may manifest itself in an increase in the residual particle mean size and sulfate concentration with distance in a track downwind of the ship.

Additionally, SO_2 can dissolve and be oxidized in cloud droplets. The effect of aqueous-phase oxidation of SO_2 would be to cause the mean residual (scavenged) particle size to increase. This in turn would cause the

supersaturation necessary to activate the particles to be lower in the next cloud forming on them. While aqueous-phase oxidation of SO_2 would modify the CCN spectra of the residual particles, the cumulative effect would be small since the original particles had already formed droplets. In any case, the effect would not be noticed in the cloud in which the aqueous-phase oxidation occurred—it would appear only in subsequent cloud formation.

Gas-to-particle conversion comprises those processes in which vapor species transfer to the particulate phase either by forming new embryonic particles through homogeneous nucleation or by condensation on preexisting particles. The vapor species that are candidates for gas-to-particle conversion in the ship track system are SO_2 and hydrocarbons emitted by the ship and H_2SO_4, which is an oxidation product of SO_2. Some gas-to-particle conversion is likely to occur in the combustion gases as they cool immediately downstream of the ship stack. This conversion involves relatively nonvolatile organic combustion products that condense on combustion particles as the temperature of the effluent gases drops rapidly, and is likely to be completed well before the ship plume reaches the cloud layer.

The background particle distribution also will be important in determining the number of new particles created by homogeneous nucleation. This potential particle source is exponentially dependent on the SO_2 concentration, and although nucleation has not been shown to be significant at background SO_2 levels, concentrations as high as 200 ppb have been observed in ship plumes (W. Hoppel 1996, personal communication). At such levels, nucleation could be a significant particle source even with high background aerosol concentrations.

Given the complexity of even the background, unperturbed aerosol–cloud–dynamic interactions, it was necessary to structure the experiment around a set of testable hypotheses in order to be able to separate and isolate individual contributing factors of the ship track phenomenon.

b. Hypotheses

The MAST experimental design was aimed at hypothesis testing. Our goal was to develop a set of hypotheses concerning the formation and life cycles of ship tracks, and then to come up with a set of measurements necessary to provide us with sufficient information to test the hypotheses. The suite of necessary observations then dictated which platforms would be needed to practically make the measurements.

Ten hypotheses were developed in early planning by the MAST science team. Figures 5 and 6 are schematic diagrams of the hypothesized processes of ship track formation. The ship track phenomenon begins with emission of various constituents into the marine atmosphere. In the figures, rectangles represent processes and ovals indicate the effect of a process on a specific constituent (up arrows for an increasing effect and down arrows for a decreasing effect). For example, the process of direct particle injection from the ship is expected to increase the CCN concentration at cloud base. Through the process of condensation, cloud droplet number concentration should increase and droplet size should decrease. The process flow continues until the observable parameter (reflectance) is changed at cloud top. The solid arrows indicate the constituent change had been observed in aircraft, ship, or satellite measurements for ship tracks prior to MAST. The experimental design described below was developed to check the previously sparse measurement set and fill in the highest-priority missing measurements.

The MAST experiment was designed around obtaining a set of measurements sufficient to test 10 hypotheses. Below, the hypotheses are grouped into four categories, and within each category, the hypotheses are ranked in order of presumed priority of influence on ship track formation.

1) Aerosol–cloud interactions and cloud microphysics
   - (i) Submicron aerosol particles from the ship stack are responsible for cloud droplet and radiative features of ship tracks.
   - (ii) Submicron aerosol particles from the water wake are responsible for cloud droplet and radiative features of ship tracks.
   - (iii) In a precipitating cloud, aerosol injection and the resulting increase in CCN act to stabilize the drop size distribution thereby reducing the number of precipitation-sized droplets and increasing the column liquid water content (LWC).
   - (iv) Gas-to-particle conversion provides a source of CCN for cloud modification down track.
   - (v) Ship-enhanced entrainment of aerosol from above the marine boundary layer enhances drop formation, reduces droplet size, and increases reflectance.
2) Boundary layer perturbations by ships
   - (i) Heat and moisture injection from ship stack enhances buoyancy and vertical motion affecting (a) cloud formation and (b) the delivery of aerosol to cloud base.
   - (ii) Mechanical generation of turbulence can enhance and perturb the ambient marine boundary layer structure and help in the formation of cloud features.
3) Cloud dynamics
   - (i) Cloud reflectance and LWC changes influence the radiation balance creating circulations that stabilize and confine the ship track region as a radiation-forced dynamic cloud.
   - (ii) Latent heat of condensation enhances vertical motion within the track and maintains its form.
4) Background environmental conditions

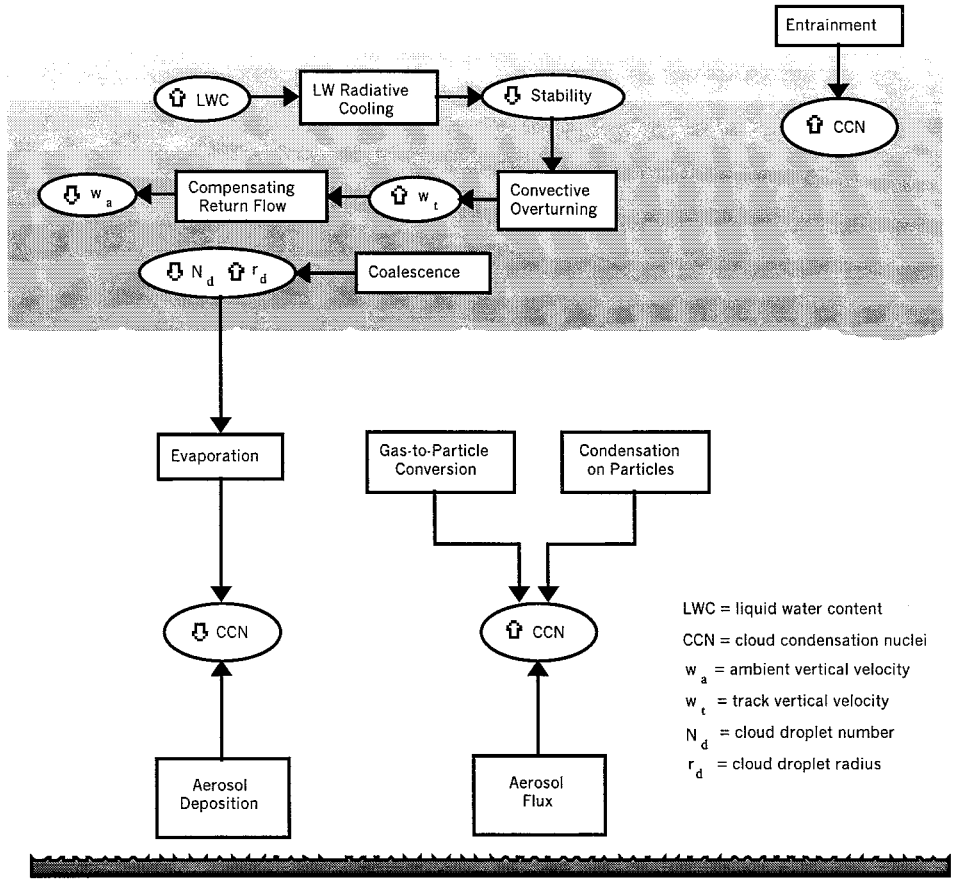

FIG. 6. Same as Fig. 5 but for down-track processes.

(i) Ship track formation requires a set of background conditions that involve small boundary layer depth, CCN concentration below a given threshold, and preexisting cloud formation mechanisms.
(ii) A decoupled marine boundary layer inhibits transport of ship effluent to upper cloud.

c. Measurement strategy for hypothesis testing

The MAST experiment tested the set of hypotheses listed above using a set of dedicated navy ships and using ships of opportunity traveling on the coastal shipping lanes. The design of measurement strategies varied somewhat depending on whether dedicated ships or ships of opportunity were being observed. The dedicated ships were operated in combinations that tested the importance of particles (direct stack injection, gas-to-particle conversion, and water wake particle production) and the role of heat and momentum release into the boundary layer. The use of a nuclear ship provided the opportunity of a ship with no particulate stack emissions, while the two conventional navy vessels provided the opportunity to test the effect of differing fuel types. Ships of opportunity were often within easy range of the research aircraft during the experiment. A wide range of ship sizes, power plant and fuel types, and steaming conditions were encountered among the ships of opportunity. The wide range of source types, as well as our ability to direct the dedicated vessels into specific areas or into a set of specific maneuvers, gives us a range of conditions under which to test the hypotheses. A detailed look at the ship characteristics and emissions is presented in Hobbs et al. (2000).

As is true for all atmospheric field programs, the conclusions drawn from the hypothesis tests depend on the environmental conditions encountered during the experiment. This initial field program was not long enough or large enough to completely investigate the wide array of meteorological conditions in which ship tracks have been observed and in which aerosols can influence cloud albedo. Therefore, MAST was designed to provide sufficient details about the primary physical processes of ship track formation, so that physically based models can be developed and predictions generated for the effects of pollutants on cloud albedo in environments not directly observed during the experiment. Case studies of ship track formation in moderately polluted (Noone 2000b) and polluted (Noone 2000a) conditions are pre-

sented, which can hopefully serve as sources of detailed information for future model studies.

1) Aerosol–cloud interactions

Testing the hypotheses in group 1 requires being able to identify and distinguish between the chemical and microphysical properties of aerosols from several potential sources: ship stack emissions, ship water wake, aerosol from above the boundary layer, and newly formed particles. A number of complementary measurements are needed. They include

- CCN concentration and supersaturation spectra;
- droplet residual aerosol size distributions and chemistry;
- cloud interstitial and out-of-cloud aerosol size distributions;
- particle thermal volatility;
- filter collections for hydrocarbon analysis;
- filter collections for major ion analysis;
- cloud drop concentration, size distribution, and effective radius; and
- liquid water content.

Hudson et al. (2000), Russell et al. (2000), and Ostrom et al. (2000) describe the particle characteristics observed in and out of ship tracks. Durkee et al. (2000b) analyze measurements selected from the entire campaign and present a test of hypotheses 1i and 1ii. They present cases where links between aerosol from specific sources and observed changes in cloud microphysics and radiative properties were observed. Hypothesis 1iii concerning the suppression of drizzle by an injection of additional aerosol is tested in Ferek et al. (2000).

2) Boundary layer perturbations by ships

For ship tracks to form in the cloud-topped marine boundary layer, whatever quantity it is that causes them (ship-generated aerosols, additional heat and moisture from the stack, mechanically generated turbulence) must be transported from the near-ship environment up to cloud level before it dissipates to background levels. Aerosols were treated in the group-1 set of hypotheses. The hypotheses in group 2 concern the effects of heat and mechanically generated turbulence on ship track formation.

Testing the atmospheric response expected from these hypotheses presents a challenge. With the exception of cloud liquid water content, direct measurement of the critical atmospheric parameters (vertical velocity and temperature) with sufficient precision is very difficult.

Necessary measurements for group-2 hypotheses include

- CCN supersaturation spectra (ship, aircraft);
- high-resolution temperature, humidity, and vertical velocity values (ship, aircraft);
- cloud droplet concentrations and size distributions; and
- environmental conditions (meteorological profiles within and above the marine boundary layer).

In addition to aircraft measurements, Hooper and James (2000) present measurements of ship plumes obtained using a lidar aboard the R/V *Glorita.*

3) Cloud dynamics

One of the more intriguing aspects of ship tracks is their persistence. They remain intact and distinct in satellite images for hundreds of kilometers downstream of the ships causing them. In addition, their dispersion over large spatial and temporal scales is surprisingly small. The two group-3 hypotheses address this persistence and lack of dispersion.

Measurements similar to those required to test the group-2 hypotheses are needed to test the group-3 set. The role of dispersion in the cloud-topped marine boundary layer is explored in Liu et al. (2000).

4) Background environmental conditions

We must recognize at the outset that it is impossible to properly test the group-4 hypotheses with a single experiment in a single location. As in all field experiments, we were limited to making our measurements under the conditions we encountered. However, we can begin charting the boundaries of the set of necessary conditions for ship track formation.

Radiosonde profiles of the boundary layer over the ocean are very scarce. It was important for the participating ships and aircraft to make as many vertical soundings as possible over as wide a geographical area as possible to sufficiently characterize the marine boundary layer.

Coakley et al. (2000) examine the large-scale aspects of ship track formation, while Liu et al. (2000) and Durkee et al. (2000a) investigate the relationship between boundary layer conditions and ship track formation. Ackerman et al. (2000), Taylor et al. (2000), and Platnick et al. (2000) look at differences between the radiative properties of the background clouds and ship tracks.

d. Modeling strategy

Numerical models are required to fulfill the complete set of objectives for MAST. Models are useful in two ways. First, they are important for improving our physical understanding of the processes behind the indirect radiative effect of pollution. Physical processes that are well understood can be quantified and parameterized in numerical models, and the models used to explore situations not encountered in the suite of observations. While the availability of dedicated vessels allowed us

TABLE 2. List of the platforms used in the MAST experiment.

Platform	Availability
University of Washington C-131A aircraft	60 h, 1–30 Jun
United Kingdom MRF C-130 aircraft	60 h, 1–30 Jun
NASA ER-2 aircraft	30 h, 1–21 Jun
Naval Research Laboratory airship	90 h, 15–29 June
Research Vessel *Glorita*	1–30 Jun
U.S. Navy ships	6–10 days
NOAA-9, -10, -11, -12 (AVHRR; TIROS Operational Vertical Sounder) satellites	Four overpasses per day
GOES-7	Half-hourly imagery
Defense Meteorological Satellite Program satellites	Two overpasses per day

to design scenarios where we were able to combine ship types and maneuvers to isolate a single variable or a set of variables, models will allow us to perform a much larger number of ''what-if'' experiments.

A five-level hierarchy of models has been developed for exploring the ship track phenomenon. In decreasing order of complexity, the models include a 3D large eddy simulation model, a two-dimensional *k*–epsilon (2D k–ϵ) model; a Lagrangian stochastic method; a Gaussian plume model; and a Lagrangian tracer model. A large-eddy simulation study by Liu et al. (2000) investigated group-2 hypotheses and is included in this special issue.

4. Platforms for hypothesis testing

A wide array of platforms was required to measure the parameters needed for testing the above hypotheses. Table 2 lists the platforms used in the field experiment in June 1994 and their availability: All platforms were equipped to measure state variables. Tables 3–7 list additional measurements made from the individual platforms.

a. Aircraft

The in situ research aircraft (UW C-131A and UK C-130) were the principal platforms for measurements of cloud and boundary layer properties in the vicinity of ship track formation. Both aircraft measured basic meteorological variables (temperature, dewpoint temperature, pressure, liquid water content, etc.); cloud and aerosol microphysical parameters; and radiation within, above, and below clouds. Detailed descriptions of the normal suite of measurements and instruments on the aircraft are available in Hobbs et al. (1991) and Rogers et al. (1995) for the UW C-131A and MRF C-130, respectively. The UW C-131A additionally made measurements of gas and aerosol chemistry. The UK C-130 was also configured to measure turbulence within the boundary layer and associated fluxes of heat, moisture, and momentum, as well as some aerosol measurements.

The ER-2 was instrumented to make high spatial, spectral, and radiometric resolution measurements of the reflectance of clouds and imbedded ship track features. These measurements supplemented the observations made from NOAA AVHRR satellite measurements of tracks during the four overpass times available each day.

The Naval Research Laboratory (NRL) airship was instrumented to make aerosol and cloud microphysics measurements as well as some observations of gas and aerosol chemistry. The operating characteristics of the airship allowed it to make measurements very near to the ships for source characterization of the ship stack plume and water wake aerosol generation.

1) UNIVERSITY OF WASHINGTON C-131A

The UW C-131A was primarily used to investigate the aerosol–cloud interactions resulting in the observed increase in ship track albedo relative to ambient cloud. Table 3 describes the instrumentation aboard the C-131A. In addition to investigators from the University of Washington, groups from the California Institute of Technology (CIT), Desert Research Institute, and the University of Rhode Island were aboard. The approach was to characterize the chemistry and microphysics of the aerosol–cloud system using several inlets and measurement techniques. Interstitial inlets (which inertially removed droplets larger than 1.75-μm radius) were used to sample the out-of-cloud aerosol and the aerosol not scavenged in cloud. A counterflow virtual impactor (CVI) inlet was used to characterize the cloud droplet residuals—the aerosol that formed cloud droplets. A number of measurements were made on samples from both types of inlets, which are summarized in Table 4.

The interstitial inlets were designed to sample aerosol particles that are smaller than cloud droplet size. Outside of cloud, most of the number population of aerosol particles was sampled with the interstitial inlets. Inside of cloud, the interstitial inlets sampled that fraction of the aerosol not scavenged into cloud droplets. There were three interstitial inlets: one for continuous measurements, and two that aspirated ambient air into chambers, allowing measurements that may take up to several minutes to be made on a single volume of air. One of these chambers is called the no-bag sampler, which is a piston expansion chamber. The other is called the big-bag chamber and is a 2.5 m^3 HDPE bag. The cycle time (filling, sampling, emptying) for the big-bag chamber is circa 5 min.

The CVI inlet sampled cloud droplets larger than approximately 5–6 μm in radius, excluding the interstitial aerosol. The droplets were evaporated, leaving behind residual aerosol particles upon which chemical (single particle analysis by SEM/EDS, hydrocarbon analysis; both carried out after the experiment) and microphysical measurements (size distributions using a PMS PCASP) were made.

Out-of-cloud and cloud interstitial aerosol size distributions were measured with several techniques and

TABLE 3. Measurements and instrumentation aboard the University of Washington C-131A.

Instrument		Range/sensitivity
	Aerosol	
Number of concentration	(GE CNC II)	$0.01 >$ Radius
Number concentration (ultrafine)	(TSI 3025)	$0.003 >$ Radius
CCN spectrometer	(UW)	$0.2 <$ Supersaturation $< 2\%$
Size spectrum	(TSI 3030)	$0.01 <$ Diameter < 0.6 μm
	(PMS LAS-200)	$0.5 <$ Diameter < 11 μm
	(PMS FSSP-300)	$0.3 <$ Diameter < 20 μm
	(PMS ASASP-X)	$0.09 <$ Diameter < 3 μm
	(PMS PCASP-100X)	$0.1 <$ Diameter < 3 μm
	(TSI DMPS)	$0.02 <$ Diameter < 0.6 μm
Salt particle mass distribution	(UW)	$0.05 <$ Diameter < 5 μm
Light scattering coefficient	(MRI 1567)	$10^{-6} < \sigma_s < 2.5 \times 10^{-3}$ m^{-1}
	Cloud	
Cloud liquid water	(Johnson–Williams and PMS-King)	$0 <$ LWC < 6 g m^{-3}
Cloud liquid water		$0.001 <$ LWC < 10 g m^{-3}
Mean droplet radius	(Gerber PVM-100)	$2 <$ Diameter < 70 μm
Cloud droplet spectrum	(PMS FSSP-100X)	$2 <$ Diameter < 47 μm
Precipitation droplet spectrum	(PMS OAP-200Y)	$300 <$ Diameter < 4000 μm
Images of cloud and precipitation droplets	(PMS OAP-2D-C & OAP-2D-P)	$C = 25\dagger\mu$m; $P = 200$-μm resolution
	Radiation	
Hemispheric (up and down) broadband solar	(Eppley PSP)	$0.3 < \lambda < 3$ μm
Hemispheric (up and down) broadband UV	(Eppley 14042)	$0.295 < \lambda < 390$ μm
Cloud absorption radiometer	(NASA Goddard Space Flight Center, UW)	13 channels $0.5 < \lambda < 2.3$ μm
	Chemistry	
	(ASRC with UW modifications)	
Cloud water samples	(UW)	$0.1 <$ mass conc. < 50 μg m^{-3}
Particulate sulfur, $SO_4^=$, NO_3^-, Cl^-, Na^+, K^+, $NH_4^+SO_2$	(TECO 43S)	$0.1 <$ conc. < 1 ppm
Ozone	(Monitor Labs 8410 A)	$0 <$ conc. < 5 ppm
NO, NO_2, NO_3	(Monitor Labs 8840, modified)	$0 <$ conc. < 5 ppm
CO	(TECO 48)	$0 <$ conc. < 50 ppm
CO_2	(modified TECO 41H and LI-COR 6262)	$0 <$ conc. < 1000 and 3000 ppm
	Supporting	
Navigation	(Litton LTM-3000)	
Global positioning system	(Trimble TNL-3000)	
Radar altimeter	(AN/APN22)	$0 < z < 6$ km
Pressure altitude	(Rosemount 830BA)	$150 < p < 1100$ mb
Total air temperature	(Rosemount 102CY2CG and 414 L Bridge)	$-60 < T < 40$ C
Static air temperature	(UW)	$-60 < T < 40$ C
Dewpoint	(Cambridge System TH73-244)	$-40 < T$d3 < 40 C
Absolute humidity	(Ophir IR-2000)	$0 <$ Humidity < 10 g m^{-3}
Air turbulence	(MRI 1120)	$0 < p$ variation < 10 cm$^{2/3}$ s^{-1}
Radiometric surface temperature	(Heimann KT19)	$8 < \lambda < 14\dagger\mu$m
	University of Rhode Island–Stockholm University	
Counterflow virtual impactor		Residuals from $r_d > 3$–4 μm
	Desert Research Institute	
CNN spectrometer		
	California Institute of Technology	
Scanning electrical mobility spectrometer		$0.005 <$ Diameter $< 0.5\dagger\mu$m

inlets to address specific questions. The CIT group used a radial scanning electrical mobility spectrometer (RCAD-SEMS) on the no-bag sampler to make rapid (circa 30 s) measurements of the aerosol size distribution in the range 0.005–0.1 μm. In addition to these measurements, UW investigators had two optical particle counters on the no-bag inlet that extended the aerosol size distribution measurements to above 1 μm.

Filter samples for aerosol chemical measurements were taken from the big-bag chamber. The concentrations of semi- and nonvolatile hydrocarbons (analyzed postexperiment at CIT), major ions, and SO_2 (analyzed at UW) were determined. Each hydrocarbon filter sample required the bag to be filled at least 3 times.

Aerosol size distributions in the big-bag chamber were determined using a scanning differential mobility analyzer. Measurements of condensation nuclei (CN), CCN, and aerosol volatility were made from chamber samples on an intermittent basis. CCN spectra measurements were made on a circa 1-s basis using the continuous interstitial inlet. Aerosol volatility measurements were also made from the continuous inlet.

The number and size distributions of residual particles were measured on the CVI inlet. Filter samples for sin-

TABLE 4. A matrix of inlets, measurements and participating groups on the UW C-131A.

Group/inlet	UW	California Institute of Technology	Desert Research Institute	University of Rhode Island
Interstitial, no bag	ASD: LAS200 0.5–13 μm, 45 s	ASD: Scanning electrical mobility spectrometer 5–100 nm, 30 s		
	ASD: ASASP 0.09–1 μm, 45 s			
Interstitial continuous	Salt counter		CCN: 1 s	
	NO_x: 200 pptv SO_2: 100 ptv O_3: 5 ppbv CO: CO_2:		Aerosol volatility	
			CN: 1 s	
Interstitial, big bag	Filter: SO_2 10 pptv 5 min	Filter: Hydrocarbons 5 min	Aerosol volatility: Intermittent	
	ASD: DMA		CNN + CN Intermittent	
Counterflow virtual impactor		Filter: Hydrocarbons Integrated	CCN: Intermittent	ASD: PCASP 0.12–10 μm, 1s
				CN: 1 s
			Aerosol volatility: Intermittent	Filter: SEM/EDAX

gle-particle chemical analysis of the residual aerosol using SEM/EDS were taken (analyzed postexperiment at the University of Rhode Island and at the University of Antwerp), as well as filter samples for hydrocarbons analyzed at CIT. CCN measurements were also made on an intermittent basis using the CVI.

2) UNITED KINGDOM METEOROLOGICAL RESEARCH FLIGHT (MRF) C-130

The primary measurements aboard the Meteorological Research Flight Hercules C-130 included turbulence, boundary layer thermodynamic structure, cloud and

TABLE 5. Measurements and instruments on board the MRF C-130.

Instrument		Range/sensitivity
	Aerosol	
Aerosol size spectrum	(PMS PCASP)	$0.1 < \text{Diameter} < 3.0$ μm
Aerosol chemical composition	(VACC − UMIST)	$0.1 < \text{Diameter} < 3.0$ μm
	Cloud	
Cloud droplet spectrum	(PMS -100)	$0.5 < \text{Diameter} < 45$ μm
Cloud condensation saturation gradient	(U.K. Meteorological Office)	
	Radiation	
Hemispheric (up and down) broadband IR	(U.K. Meteorological Office)	$4 < \lambda < 50$ μm
Hemispheric (up and down) broadband solar	(Eppley PSP)	$0.3 < \lambda < 3$ μm
Hemispheric (up and down) broadband near-IR	(Eppley PSP)	$0.7 < \lambda < 3$ μm
Atmospheric radiance filter wheel radiometer	(U.K. Meteorological Office)	$0.5 < \lambda < 15$ μm
Microwave radiation	(U.K. Meteorological Office)	$\nu = 89$ and 257 GHz
	Supporting	
Inertial navigation	(Honeywell H423)	
Global positioning system	(Navstar XR5)	
Radar altimeter	(Honeywell YG9000D1)	$0 < z < 1525$ m
Static pressure	(Rosemount 1201F)	
Total air temperature	(Rosemount 102BL/AL)	
Dewpoint (thermoelectric)	(General Eastern 1011B)	
Absolute humidity (Lyman-α absorption and fluorescence)	(U.K. Meteorological Office)	
Total water content (Lyman-α absorption)	(U.K. Meteorological Office)	
In-cloud temperature	(U.K. Meteorological Office)	
Radiometric surface temperature	(Heimann)	$8 < \lambda < 14$ μm

TABLE 6. Measurements and instruments on board the NASA ER-2.

Instrument		Range/sensitivity
MODIS airborne simulator	(NASA)	11 channels $0.66 < 1 < 12.0\dagger\mu$m
Cloud Lidar System	(NASA)	$\lambda = 0.532$ and $1064\dagger\mu$m
RC-10 camera	(NASA)	

aerosol microphysics, and multispectral radiation measurements. The long range (8–9 h) of the Hercules provided both the needed flexibility in designing mission scenarios and the ability to observe ship tracks at long distances from the coast (up to 1000 km).

In addition to the normal suite of measurements made from the C-130, a group from the University of Manchester, United Kingdom, measured aerosol size distributions and thermal volatility (O'Dowd and Smith 1993). These measurements were used to estimate the chemical composition of the accumulation-mode aerosol. Table 4 summarizes the measurements and instruments on the MRF C-130.

3) NATIONAL AERONAUTICS AND SPACE ADMINISTRATION (NASA) ER-2

The ER-2 carried high spatial, spectral, and radiometric resolution instruments to measure the reflectance of ship track features and surrounding clouds. The ER-2 supplemented the remote sensing observations of ship tracks made from NOAA AVHRR satellites during the four overpass times available each day. The NASA Moderate Resolution Imaging Spectroradiometer (MODIS) Airborne Simulator measured radiance in 11 wavelength bands from red-visible to the thermal infrared at a spatial resolution of 50 m over a swath width of 37 km. The ER-2 also carried the Cloud Lidar System to measure cloud-top topography. Two high-resolution camera systems provided cloud and ship images. These measurements are summarized in Table 6.

4) NRL AIRSHIP

The NRL airship was instrumented to make aerosol and cloud microphysics measurements as well as some gas and aerosol chemistry. Table 7 lists the instrumentation aboard the airship. The operating characteristics of the airship allowed it to make measurements very near to the ships for characterization of the ship stack plume and water wake aerosol generation (Frick and Hoppel 2000).

A differential mobility analyzer and an optical Classical Scattering Aerosol Spectrometer Probe made aerosol measurements. NRL made gaseous measurements of SO_2, NO_x, ozone; and Texas Tech University measured gas-phase peroxides, formaldehyde, and ammonia. A GERBER PVM-100 for cloud liquid water and radon measurements supplemented standard thermodynamic measurements. The University at Albany, State University of New York, analyzed liquid water chemistry for major ions and peroxides.

b. Ships

1) R/V *GLORITA*

The research vessel R/V *Glorita* made slow transits under ship tracks generated by dedicated ships and ships

TABLE 7. NRL airship instrumentation.

Instrument		Range/sensitivity
Aerosol		
NRL DMA size spectrometer (operating in 2-min scanning mode)		$0.005 <$ Radius < 0.6 μm
Optical size spectrometer	(PMS CSASP-100HV)	$0.30 <$ Radius < 25 μm
TSI condensation particle counter	(Model 3022)	Radius > 0.003 μm
Trace gas		
SO_2 analyzer	(TECO Model 43S)	0.1 ppb
NO_x analyzer	(Dasibi Model 2108)	2.0 ppb
Ozone	(Dasibi Model 1008)	1.0 ppb
Supporting		
Radon (as airmass tracer)		1 pCi m^{-3}
Cloud liquid water		0.001–10 g m^{-3}
Mean droplet radius	(Gerber PVM-100)	2–70 μm
Pressure		3 mb
Temperature		0.2°C
Dewpoint temperature	(General Eastern 1200 APS)	0.3°C
IR surface temperature	(Everest Model 4000 ALCS)	0.5°C
GPS navigation system		
SUNYA ASRC		
Cloud liquid water chemistry (major ions and peroxides)		
Texas Tech University		
Using diffusion scrubber techniques	Gas-phase peroxides	
	Formaldehyde	
	Ammonia	

TABLE 8. Measurements and instruments on the R/V *Glorita.*

Instrument
The Pennsylvania State University
Cloud doppler radar (95 GHz)
Rawinsondes
Ceilometer
Microwave radiometer
Atmospheric fluxes
Naval Research Laboratory
Volume imaging lidar (1.06 μm)
Desert Research Institute–City College, New York
CCN spectrometer
Condensation nuclei concentration
Los Alamos National Laboratory
Tethersonde Profiles
Ceilometer
Applied Physics Laboratory, The Johns Hopkins University
Test operations
Track reconstruction
Communications

of opportunity. The *Glorita* was instrumented for measurements of in situ meteorological parameters including turbulence and vertical profiles of temperature, water vapor, and wind (Table 8). Additional remote measurements from the ship included a microwave radiometer and a 94-GHz Doppler radar system (operated by The Pennsylvania State University) that provided cloud mapping, including circulation characteristics. To study the aerosol plume, the Naval Research Laboratory operated an imaging lidar that mapped out the aerosol backscatter behind the target ships. Los Alamos National Laboratory operated a tethered sounding system to produce high-resolution thermodynamic analyses. The *Glorita* was also equipped with aerosol and CCN measuring systems to provide surface-based observations when aircraft were unavailable. Groups from the Desert Research Institute operated a CCN spectrometer for half the experiment; and City College, New York, made CN measurements from the vessel.

2) DEDICATED SHIPS

Dedicated ships provided a measure of control to the field measurements. These ships were operated in coordination with the primary measurement platforms. The mission scenarios made use of the prevailing winds and current cloud conditions. The suite of ships included diesel, steam turbine, gas turbine, and nuclear power plants. Table 9 lists the ships and their dates of operations. The USS *Truxtun* and USS *Kansas City* also launched radiosondes in support of MAST.

3) SHIPS OF OPPORTUNITY

Ships of opportunity were investigated when dedicated ships were unavailable or when they were producing particularly interesting tracks. The wide range of ship types, sizes, and cruising conditions allowed us to operate in a fairly wide range of environmental conditions. In many cases, radio contact was established with the ship; and its fuel type, operating conditions, and other information were relayed to the operations center. In other cases, the ship operator was contacted and similar information was obtained for the normal operating characteristics of the ship in question. Table 10 lists all of the ships of opportunity investigated during the experiment.

c. Satellites

Satellite data from *NOAA-9, -10, -11,* and *-12* AVHRR was collected in real time during the experiment. Analysis of the visible and infrared channels provided the best detection of ship effects (especially channel-3, 3.7-μm wavelength). Defense Meteorological Satellite Program data were also available in real time, providing high-resolution visible data (about 0.5 km) and microwave data from the special sensor microwave/imager instrument. *GOES-7* data were available over network connections and in loop form for weather forecasting needs.

5. MAST operations summary

The MAST operations center was located at the Naval Postgraduate School in Monterey, California. Real-time analysis of AVHRR and GOES satellite imagery was used to plan aircraft and R/V *Glorita* operations. Im-

TABLE 9. U.S. Navy ships participating in MAST.

Vessel	Propulsion system	Dates of operation	Airborne platforms
USS *Copeland* FFG 25 (Perry class frigate)	Gas turbine	8–9 Jun	UW C-131
USS *Safeguard** ARS 50 (fleet support ship)	Diesel	12–13 Jun	UW C-131 MRF C-130
USS *Kansas City* AOR 3 (replenishment oiler)	Steam turbine	21–22 Jun	UW C-131 MRF C-130
USS *Mount Vernon* LSD 39 (dock landing ship)	Steam turbine	28–30 Jun	UW C-131 Airship
USS *Truxtun* CGN 35 (Belknap class cruiser)	Nuclear	28–29 Jun	UW C-131 Airship

* Ship track observed.

TABLE 10. Ships of opportunity investigated during the MAST experiment.

Vessel	Propulsion system	Dates of operation	Airborne platforms
*Monterrey**	Diesel	1 Jun	UW C-131A
Sierra Madre	Steam turbine	1 Jun	UW C-131A
Pu He	Diesel	1 Jun	UW C-131A
*Keystone Canyon**	Steam turbine	8 Jun	MRF C-130
*Fremo Scorpius**	Diesel	8 Jun	UW C-131A
*Samuel H. Armacost**	Diesel	8 Jun	UW C-131A
*Hyundai Duke**	Diesel	8 Jun	MRF C-130
*Newport Bridge**	Diesel	9 Jun	MRF C-130
Toluca	Diesel	9 Jun	UW C-131A
*Ever Gather**	Diesel	9 Jun	MRF C-130
*Brazil Vitoria**	Diesel	11 Jun	UW C-131A, MRF C-130, ER-2
*Kurama**	Diesel	11 Jun	MRF C-130, ER-2
*Skaugran**	Diesel	11 Jun	UW C-131A, ER-2
*Moku Pahu**	Diesel	12 Jun	UW C-131A
*Sanko Peace**	Diesel	13 Jun	MRF C-130
USS *Abraham Lincoln*	Nuclear	15 Jun	UW C-131A
USS (unidentified frigate)	Gas turbine	15 Jun	UW C-131A
Direct Kookaburra	Diesel	16 Jun	MRF C-130
Gold Bond Trailblazer	Diesel	17 Jun	NRL airship
Bosphorus Bridge	Diesel	17 Jun	UW C-131A, MRF C-130
Sea Pearl	Diesel	19 Jun	NRL airship
Unidentified ship		20 Jun	NRL airship
*Cap May**	Diesel	21 Jun	MRF C-130, ER-2
Mathilde Maersk	Diesel	26 Jun	NRL airship
*Axel Maersk**	Diesel	27 Jun	MRF C-130
*Tai He**	Diesel	27 Jun	UW C-131A, MRF C-130
*Ever Genius**	Diesel	28 Jun	MRF C-130, ER-2
*Bremmen Express**	Diesel	28 Jun	NRL airship
*Star Livorno**	Diesel	29 Jun	UW C-131A, ER-2
*Hanjin Barcelona**	Diesel	29 Jun	UW C-131A, MRF C-13
*NYK Sunrise**	Diesel	30 Jun	UW C-131A, ER-2

* Ship track observed.

agery was often used to radio recommended modifications of aircraft plans to the mission scientist on the aircraft. In several cases this resulted in observations of ship effects that would have been missed by the preflight mission plan.

The meteorological conditions during June 1994 were significantly different than expected from the climatological norm. Typically, the persistent summertime subtropical high-pressure system sets up in early June over the eastern North Pacific, initiating alongshore flow and the well-known stratocumulus cloud sheet off the California coast. However, in 1994 active troughs repeatedly suppressed the subtropical high. As these troughs moved inland, offshore flow resulted and the stratus cloud system was frequently forced more than 300 km offshore. The MAST aircraft and research vessel were therefore limited, especially early in the month, due to lack of cloud within the range of operations.

In spite of the anomalous weather conditions, many tracks formed in the eastern North Pacific during MAST. Figure 7 shows all the ship tracks observed in AVHRR imagery during June 1994. A manual analysis scheme was used to indicate the head position (dot) and track orientation. The pattern in Fig. 7 is determined by the combination of cloud cover and shipping traffic distributions. The pattern of shipping routes is clearly dominated by great circle routes between eastern Asia ports and San Francisco, Los Angeles, and the Panama Canal. Some shipping activity along the California coast is also apparent. The void area west of Oregon and Washington is partly the result of reduced ship traffic and suppression of the stratus deck during June 1994 by closed low-pressure circulation aloft.

6. Conclusions

The compilation of papers in this special issue represents the first wave of analyses from the MAST experiment. Our aim was to use ship tracks as an analog for the effects of anthropogenic pollution on cloud albedo, and to investigate the processes behind the effects. Investigating ship tracks provided us with an opportunity to carry out as controlled an experiment as we are likely to achieve in the real atmosphere to investigate the processes underlying the indirect radiative effect of aerosols on clouds. The information contained in this special issue can serve as a point of departure for further studies.

We were able to conclusively resolve many of the hypotheses we aimed to test. With the exception of hypothesis 1iv (for which analysis is currently underway), the group-1 and -2 hypotheses were largely resolved.

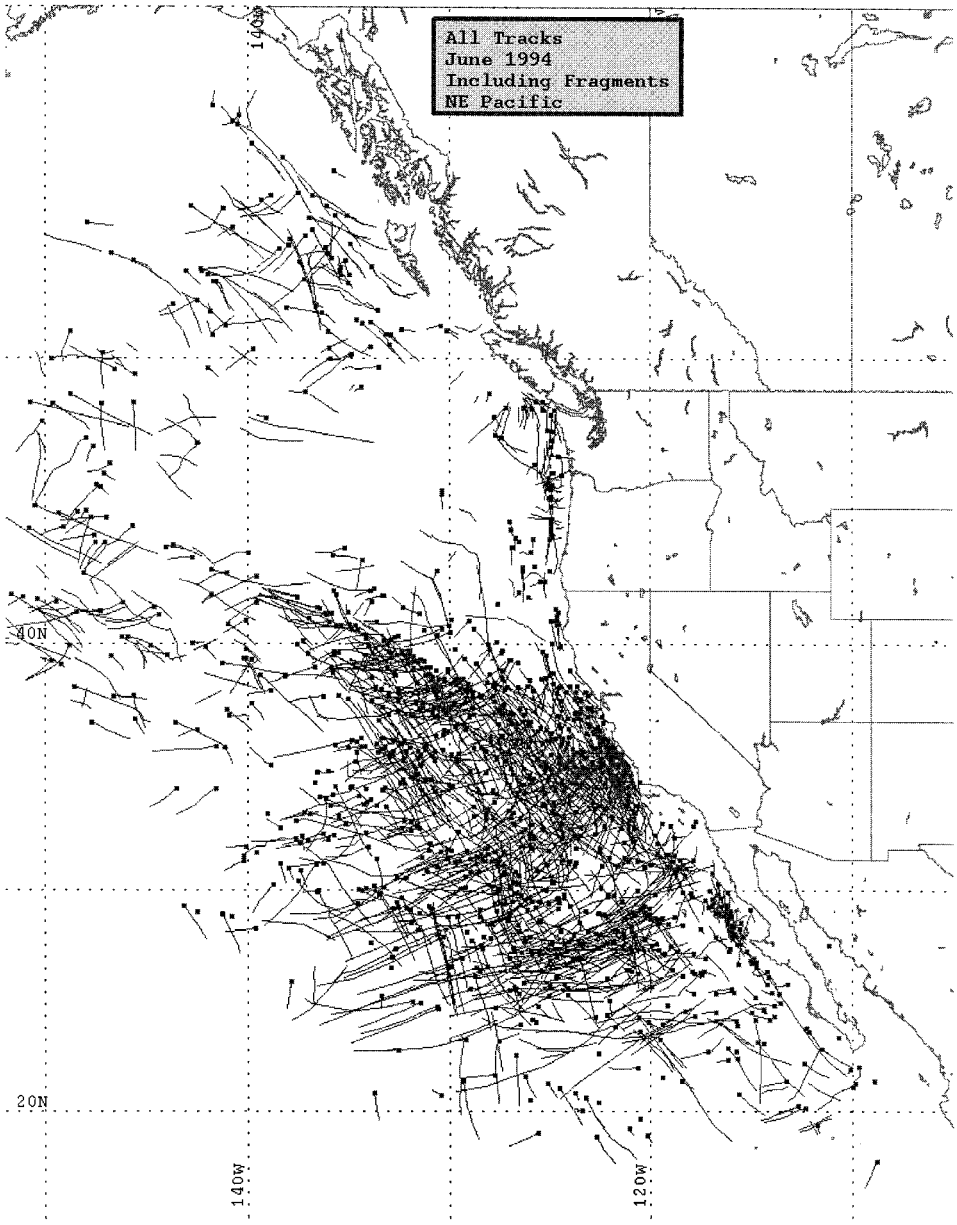

FIG. 7. Map of the distribution of the ship tracks observed in satellite imagery during Jun 1994.

While the group-3 hypotheses were not as conclusively tested, we can say that such dynamical influences are not a necessary prerequisite for formation and maintenance of ship tracks. The group-4 hypotheses were not completely tested; on the other hand, as they are stated it would be effectively impossible to test them in a strict sense. As a result of MAST, we were able to at least describe the boundary conditions in which ship tracks form in a comprehensive fashion.

We are very pleased with the outcome of the experiment. In hindsight, some of the hypotheses could have been more properly stated to aid stringent testing. It also would have been valuable to do more missions where ships *not causing ship tracks* were investigated to better characterize the negative situation. We also did not perform any in situ missions at night. Even in the best of conditions, these kinds of missions are risky, given the limited number of operation hours each of the platforms had and the desire to investigate as many different cases of ship tracks as possible. However, given the fact that the weather situation during June 1994 was far from the optimum for observing ship tracks, these shortcomings do not stop us from considering the experiment to have been quite successful.

Acknowledgments. Vince Huth, Operations Manager at the Monterey Airport, was extermely helpful in setting up the necessary facilities for operating the UW C131A and MRF C130. Kurt Nielsen provided the worldwide ship track observations. MAST was principally funded by the Office of Naval Research Accelerated Research Initiative, called the Surface Ship Cloud Effects Project.

REFERENCES

Ackerman, A. S., O. B. Toon, J. P. Taylor, D. W. Johnson, P. V. Hobbs, and R. J. Ferek, 2000: Effects of aerosols on cloud albedo: Evaluation of Twomey's parameterization of cloud susceptibility using measurements of ship tracks. *J. Atmos. Sci.,* **57,** 2684–2695.

Albrecht, B. A., 1989: Aerosols, cloud microphysics, and fractional cloudiness. *Science,* **245,** 1227–1230.

Ayers, G. P., and T. V. Larson, 1990: Numerical study of droplet size dependent chemistry in oceanic, wintertime stratus cloud at southern mid-latitudes. *J. Atmos. Chem.,* **11,** 143–167.

Bowley, C. J., 1967: Comments on atmospheric requirements for the genesis of anomalous cloud lines. *J. Atmos. Sci.,* **24,** 569–597.

Charlson, R. J., J. E. Lovelock, M. O. Andreae, and S. G. Warren, 1987: Oceanic phytoplankton, atmospheric sulphur, cloud albedo and climate. *Nature,* **326,** 655–661.

——, S. E. Schwartz, J. M. Hales, R. D. Cess, J. A. Coakley Jr., J. E. Hansen, and D. J. Hofmann, 1992: Climate forcing by anthropogenic aerosols. *Science,* **255,** 423–430.

Coakley, J. A., Jr., R. L. Bernstein, and P. A. Durkee, 1987: Effect of ship-stack effluents on cloud reflectivity. *Science,* **237,** 1020–1022.

——, and Coauthors, 2000: The appearance and disappearance of ship tracks on large spatial scales. *J. Atmos. Sci.,* **57,** 2765–2778.

Conover, J. H., 1966: Anomalous cloud lines. *J. Atmos. Sci.,* **23,** 778–785.

Durkee, P. A., R. E. Chartier, A. Brown, E. J. Trehubenko, C. Skupniewicz, K. E. Nielsen, S. Platnick, and M. D. King, 2000a: Composite ship track characteristics. *J. Atmos. Sci.,* **57,** 2542–2553.

——, and Coauthors, 2000b: The impact of ship-produced aerosols on the microstructure and albedo of warm marine stratocumulus clouds: A test of MAST hypotheses 1i and 1ii. *J. Atmos. Sci.,* **57,** 2554–2569.

Evans, M. E., 1992: Analysis of ship tracks in cloudiness transition regions. M.S. thesis, Department of Meteorology, Naval Postgraduate School, 93 pp. [Available from Department of Meteorology, Naval Postgraduate School, 589 Dyer Rd., Monterey, CA 93943.]

Falkowski, P. G., Y. Kim, Z. Kolber, C. Wilson, C. Wirick, and R. Cess, 1992: Natural versus anthropogenic factors affecting low-level cloud albedo over the North Atlantic. *Science,* **256,** 1311–1313.

Ferek, R. J., D. A. Hegg, P. V. Hobbs, P. A. Durkee, and K. E. Nielsen, 1998: Measurements of ship-induced cloud tracks off the Washington coast. *J. Geophys. Res.,* **103,** 23 199–23 206.

——, and Coauthors, 2000: Drizzle suppression in ship tracks. *J. Atmos. Sci.,* **57,** 2707–2728.

Frick, G. M., and W. A. Hoppel, 2000: Airship measurements of ship's exhaust plumes and their effect on marine boundary layer clouds. *J. Atmos. Sci.,* **57,** 2625–2648.

Han, Q., W. B. Rossow, and A. A. Lacis, 1994: Near-global survey of effective droplet radii in liquid water clouds using ISCCP data. *J. Climate,* **7,** 465–497.

Hansen, J., and Coauthors, 1995: Low-cost long-term monitoring of global climate forcings and feedbacks. *Climatic Change,* **31,** 247–271.

Hegg, D. A., 1991: Particle production in clouds. *Geophys. Res. Lett.,* **18,** 995–998.

Hindman, E. E., and R. Bodowski, 1994: A marine stratus layer modified by ship-produced CCN and updrafts. Preprints, *Sixth WMO Scientific Conference on Weather Modification,* Siena, Italy, WMO-TD-No. 596.

Hobbs, P. V., L. F. Radke, J. H. Lyons, R. J. Ferek, D. J. Coffman, and T. J. Casadevall, 1991: Airborne measurements of particle and gas emissions from the 1990 volcanic eruptions of Mount Redoubt. *J. Geophys. Res.,* **96,** 18 735–18 752.

——, and Coauthors, 2000: Emissions from ships with respect to their effects on clouds. *J. Atmos. Sci.,* **57,** 2570–2590.

Hooper, W., and J. James, 2000: Lidar observations of ship-spray plumes. *J. Atmos. Sci.,* **57,** 2649–2655.

Houghton, J. T., L. G. Meira Filho, B. A. Callander, N. Harris, A. Kattenberg, and K. Maskell, Eds., 1996: *Climate Change 1995: The Science of Climate Change.* Cambridge University Press, 339 pp.

Hudson, J. G., T. J. Garrett, P. V. Hobbs, S. R. Strader, Y. Xie, and S. S. Yum, 2000: Cloud condensation nuclei and ship tracks. *J. Atmos. Sci.,* **57,** 2696–2706.

Kim, Y., and R. D. Cess, 1993: Effect of anthropogenic sulfate aerosols on low-level cloud albedo over oceans. *J. Geophys. Res.,* **98,** 14 883–14 885.

King, M. D., L. F. Radke, and P. V. Hobbs, 1993: Optical properties of marine stratocumulus clouds modified by ships. *J. Geophys. Res.,* **98,** 2729–2739.

Kuciauskas, A., P. A. Durkee, C. Skupniewicz, and K. E. Nielsen, 1993: Radiative characteristics of ship tracks at night. *Proc. Cloud Impacts on DOD Operations and Systems (CIDOS–93),* Fort Belvoir, VA, 263–269.

Leaitch, W. R., G. A. Isaac, J. W. Strapp, C. M. Banic, and H. A. Weibe, 1992: The relationship between cloud droplet number concentrations and anthropogenic pollution: Observations and climatic implications. *J. Geophys. Res.,* **97,** 2463–2474.

Liu, Q., Y. L. Kogan, D. K. Lilly, D. W. Johnson, G. E. Innis, P. A. Durkee, and K. E. Nielsen, 2000: Modeling of ship effluent transport and its sensitivity to boundary layer structure. *J. Atmos. Sci.,* **57,** 2779–2791.

Millman, T., 1992: A temporal analysis of east Pacific and east Atlantic ship tracks. M.S. thesis, Department of Meteorology, Naval Postgraduate School, 69 pp. [Available from Department of Meteorology, Naval Postgraduate School, 589 Dyer Rd., Monterey, CA 93943.]

Noone, K. J., and Coauthors, 1992: Changes in aerosol size and phase distributions due to physical and chemical processes in fog. *Tellus,* **44B,** 489–504.

——, and Coauthors, 2000a: A case study of ship track formation in a polluted marine boundary layer. *J. Atmos. Sci.,* **57,** 2729–2747.

——, and Coauthors, 2000b: A case study of ships forming and not forming tracks in moderately polluted clouds. *J. Atmos. Sci.,* **57,** 2748–2764.

O'Dowd, C. D., and M. H. Smith, 1993: Physicochemical properties of aerosols over the northeast Atlantic: Evidence for wind speed-related submicron sea-salt aerosol production. *J. Geophys. Res.,* **98,** 1137–1149.

Ostrom, E., K. J. Noone, and R. A. Pockalny, 2000: Cloud droplet residual particle microphysics in marine stratocumulus clouds observed during the Monterey Area Ship Track Experiment. *J. Atmos. Sci.,* **57,** 2671–2683.

Platnick, S., and Coauthors, 2000: The role of background cloud microphysics in the radiative formation of ship tracks. *J. Atmos. Sci.,* **57,** 2607–2624.

Radke, L. F., J. A. Coakley Jr., and M. D. King, 1989: Direct and remote sensing observations of the effects of ships on clouds. *Science,* **246,** 1146–1149.

Rogers, D. P., D. W. Johnson, and C. A. Friehe, 1995: The stable internal boundary layer over a coastal sea. Part I: Airborne measurements of the mean and turbulence structure. *J. Atmos. Sci.,* **52,** 667–683.

Russell, L. M., K. J. Noone, R. J. Ferek, R. A. Pockalny, R. C. Flagan,

and J. H. Seinfeld, 2000: Combustion organic aerosol as cloud condensation nuclei in ship tracks. *J. Atmos. Sci.,* **57,** 2591–2606.

Schwartz, S. E., 1988: Are global cloud albedo and climate controlled by marine phytoplankton? *Nature,* **336** (6198), 441–445.

Taylor, J. P., M. P. Glew, J. A. Coakley Jr., W. R. Tahnk, S. Platnick, P. V. Hobbs, and R. J. Ferek, 2000: Effects of aerosols on the radiative properties of clouds. *J. Atmos. Sci.,* **57,** 2656–2670.

Twomey, S., 1974: Pollution and the planetary albedo. *Atmos. Environ.,* **8,** 1251–1256.

——, H. B. Howell, and T. A. Wojciechowski, 1968: Comments on ''Anomalous cloud lines.'' *J. Atmos. Sci.,* **25,** 333–334.